

Article

Artificial Neural Network for Assessment of Energy Consumption and Cost for Cross Laminated Timber Office Building in Severe Cold Regions

Qi Dong ^{1,2}, Kai Xing ^{1,2,*} and Hongrui Zhang ^{1,2} 

¹ School of Architecture, Harbin Institute of Technology, Harbin 150001, China; dongqi@hit.edu.cn (Q.D.); zhhr_hit@163.com (H.Z.)

² Heilongjiang Cold Region Architectural Science Key Laboratory, Harbin 150001, China

* Correspondence: xingkai@hit.edu.cn; Tel.: +86-451-8628-1135

Received: 30 November 2017; Accepted: 28 December 2017; Published: 30 December 2017

Abstract: This paper aims to develop an artificial neural network (ANN) to predict the energy consumption and cost of cross laminated timber (CLT) office buildings in severe cold regions during the early stage of architectural design. Eleven variables were selected as input variables including building form and construction variables, and the values of input variables were determined by local building standards and surveys. ANNs were trained by the simulation data and Latin hypercube sampling (LHS) method was used to select training datasets for the ANN training. The best ANN was obtained by analyzing the output variables and the number of hidden layer neurons. The results showed that the ANN with multiple outputs presented better prediction performance than the ANN with single output. Moreover, the number of hidden layer neurons in ANN should be greater than five and preferably 10, and the best mean square error (MSE) value was 1.957×10^3 . In addition, it was found that the time of predicting building energy consumption and cost by ANN was 80% shorter than that of traditional building energy consumption simulation and cost calculation method.

Keywords: cross laminated timber; artificial neural network; energy consumption; cost; office building; severe cold regions

1. Introduction

Compared with other industries, the energy consumption of the construction industry is the largest [1]. The construction industry not only consumes a large amount of energy and natural resources in the world, but also has a significant impact on climate change and greenhouse gas emissions [2]. Its energy consumption accounts for 35% of the total energy consumption [3], and its carbon emission accounts for one third [4].

Office buildings are the largest energy consumption buildings in all types of buildings [5]. Owing to the growing demand of social development, the number of office buildings has increased dramatically. Office building consumed 172.6 billion kW·h of electricity, and its area reached 890 million m² at the end of 2007 in China [6]. Nowadays, to pursue comfortable office environment and work efficiency, the utilization of office air conditioning is much higher than other buildings. However, the utilization of energy is coarse, which leads to a great waste of energy. Therefore, how to reduce the energy consumption of office buildings has become an urgent problem to be solved. In addition, in severe cold regions the energy consumption of office buildings is much higher than other regions.

The building envelope plays a dominating role in building energy efficiency performance [7], and it is therefore of great significance to improve the performance indicators of building envelope for saving energy and reducing carbon emission [8]. Woods are widely used in building envelopes

because the heat transfer coefficient of woods are lower than that of concrete. The energy consumption and carbon emissions of wood-framed buildings are significantly lower than those of concrete-framed buildings [9].

Cross laminated timber (CLT) is a structural material, which is mainly used for the multi-storey buildings' load-bearing walls and floors [10]. It is usually made of small diameter timbers and low-value woods infected by insects [11]. The strength and stiffness of the laminated timber can be greatly improved by gluing several layers of woods to form the cross adhesive layers [12]. Not only can CLT meet the requirements of the building structure, but also can enhance the beauty of buildings, save the cost of structures and pick up the construction speed [10]. In addition, since CLT is made of laminated boards, the energy disappears with the friction of the boards during the earthquake. So, it also has a good seismic performance [13]. As early as 1990, there were some researches about laminated timber [11]. For example, there were studies about the mechanical properties and corrosion resistance of laminated timbers [14]. CLT is very popular because of the large amount of lumber, which can also be recycled. The use of CLT is in line with the requirements of sustainable development [15]. For the building life cycle, CLT, compared to steel sandwich panels, can reduce 80% energy consumption in the operating period [16]. However, there is always a negative correlation between the cost of building and the building energy consumption. Hence, architects have to balance both of the building cost and energy performance in CLT office building design [17].

Building energy consumption and building cost are two important indexes of building performance [18]. Valdiserri et al. evaluated the economy of the energy saving retrofit schemes for building envelope based on payback period. They found that the government policies and the climate of the building location had a significant impact on the payback period [19]. Song et al. analyzed the influences of the six envelope parameters on the thermal response to the envelope. It was found that the infiltration and the thermal performance of exterior walls and windows are important parameters affecting the cooling load of buildings [20]. Gustafsson et al. evaluated the energy renovation packages based on life cycle cost and life cycle assessment. Through the ways of renovation in the study, office buildings can reduce 77% of building energy consumption and 19% of the cost over 30 years [21]. Balionis et al. presented an assessment model for multi-storey office buildings based on the comprehensive evaluation of building energy consumption, investment, carbon emissions, thermal comfort and other building performance indicators by computer simulation [22]. All of the above studies have used computational methods to predict building energy consumption or calculate the construction cost. However, it is difficult to obtain the results of building energy consumption prediction and construction cost calculation simultaneously. This is because most of the existing computational softwares can only calculate one target variable. In addition, in the process of simulation or calculation, it is very complicated and time-consuming to establish a prediction model. Therefore, building energy consumption prediction and cost calculation are inefficient.

ANN is gradually being used more frequently in architectural design to predict the building performances [23,24], which was considered as a promising way to instead the utilization of building performance simulation tools [25]. It can help architects make a preliminary estimation of building performances by inputting several simple parameters in the early stage of architectural design and it can save the unnecessary modeling time and improve the efficiency of architectural design. The ANN is widely studied because of its simple operation and more accurate prediction performance [26], accounting for 41% of the studies on artificial intelligence learning algorithm for building performance prediction [27].

ANN is a machine learning tool which is used to solve nonlinear statistical problems based on biological neural network [27]. The structure of a typical ANN is composed of input, hidden and output layers which are interconnected [28]. ANNs correlate the input and output data by learning the historical data [23], which could calculate the non-linear correlation between inputs and outputs. They can also reduce the calculation time dramatically [29]. In previous studies, ANNs were used to predict the cooling energy consumption [30,31], heating energy consumption [32,33], electricity

consumption [34,35], thermal comfort [36] and the cost [37–39]. However, there are lots of researches on building performance prediction in other climatic regions [40–43], and few regarding severe cold regions. Affected by the cold climate, the building form and the thermal performances of envelopes in the severe cold regions are different from that of other climate regions. Building energy consumption and cost are also different from that of other climate regions. Therefore, it is necessary to increase the investment into the research of the prediction of building energy consumption and cost in severe cold regions. In addition, there are many studies on the ANNs of single output variables, and less researches on ANNs with multiple output variables. In summary, based on the typical form model of office buildings in severe cold regions, the paper aims to establish an ANN to help architects make a preliminary estimation of energy consumption and cost of CLT office buildings in severe cold regions by inputting several simple parameters during the early stage of architectural design. The performances of the ANN with multiple output variables is discussed, which will provide the reference for future researches.

2. Methods

2.1. The Framework

In this paper, an ANN was implemented by coupling EnergyPlus (Version 8.5, United States Department of Energy and Lawrence Berkeley National Laboratory, Washington, DC, USA and Berkeley, CA, USA), Grasshopper (Version 5.12, Robert McNeel Associates, Seattle, WA, USA) and the neural network toolbox of MATLAB (R2016a, MathWorks, Natick, MA, USA) to predict the energy consumption and the construction cost of CLT office buildings as presented in Figure 1.

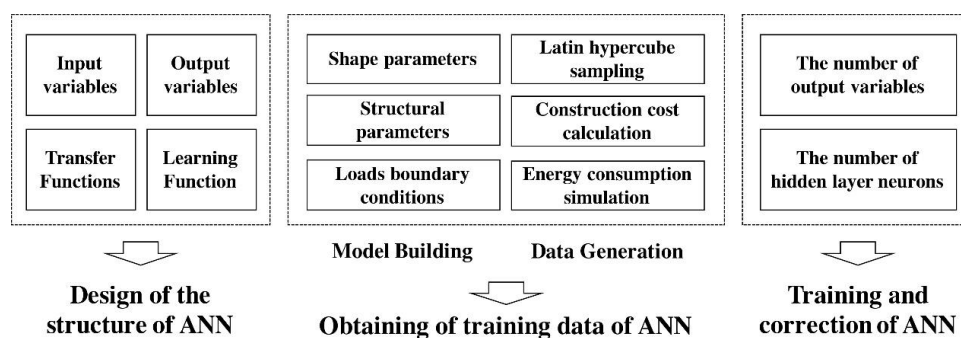


Figure 1. The framework of this paper.

Firstly, the structure of ANN was designed including a selection of input and output variables, determination of transfer and learning functions. Then, the parametric model of CLT office building with typical morphological features in severe cold regions was developed by Grasshopper.

The parameters of input variables could be easily modified to facilitate simulations and calculations in different situations. The boundary conditions of building energy consumption simulation and construction cost calculation, including thermal properties of building envelope materials, equipment and lighting loads, occupancy schedules, the prices of structure and so on, were obtained from the local standards and survey. The simulations of building energy consumption and construction cost were performed using the parametrical model coupling EnergyPlus and Grasshopper. Latin hypercube algorithm was used to sampling the input parameters.

The ANN was trained by the simulation results using MATLAB. The performances of ANNs with various numbers of output variables and hidden layer neurons are discussed below. Finally, the ANN with best performance is proposed.

2.2. Design of the Structure of ANN

The building energy consumption and construction cost were determined as output variables of the ANN in this paper. Eleven variables which could be easily determined by architects in the early stage of architectural design were selected as the input variables of the ANN. The inputs variables included 6 building form variables and 5 building construction variables as showed in Table 1.

Table 1. Input and output variables.

Type of Variable	Variable	Unit	Time Step
Input variables	Aspect ratio (length/width)	-	0.01
	North window to wall ratio	-	0.01
	South window to wall ratio	-	0.01
	East window to wall ratio	-	0.01
	West window to wall ratio	-	0.01
	Number of floors	-	1
	Thickness of exterior wall insulation layer	mm	1
	Thickness of roof insulation layer	mm	1
	Thickness of exterior wall structural layer	mm	1
	Type of external wall insulation material	-	-
	Type of roof insulation material	-	-
Output variables	Construction cost	yuan	1
	Building energy consumption	kW·h/m ²	0.001

BP (Back Propagation) ANN is a feedforward neural network, and it is widely used as its excellent performance [44]. In this paper, BP ANN with one hidden layer was applied to predict building energy consumption and cost performances. The paper selected the “Tansig” function as the transfer function between the input layer and the hidden layer, and selected the “purelin” function as the transfer function between the hidden layer and the output layer. In addition, the Levenberg–Marquardt algorithm was used to train the ANN.

2.3. Calculation of Building Performances

2.3.1. The Simulation of Energy Consumption

The building energy consumption evaluation focused on the operation phase which is of great importance and accounts for 70–80% of the total building energy consumption in life cycle assessment. The energy consumption included heating, cooling, equipment and lighting energy consumption as shown in Equation (1):

$$E = E_{he} + E_{co} + E_{eq} + E_{li} \quad (1)$$

where E is the total energy consumption (kW·h/m²), E_{he} is the heating energy consumption (kW·h/m²), E_{co} is the cooling energy consumption (kW·h/m²), E_{eq} is the equipment energy consumption (kW·h/m²), E_{li} is the lighting energy consumption (kW·h/m²).

The building energy consumption simulation tool used in this paper is EnergyPlus—an energy simulation software that integrates load, equipment and system models. The smallest time step of simulation is seconds. EnergyPlus adopts the reaction coefficient method to simulate the heat transfer process of the building envelope and it calculates the energy consumption load and the indoor temperature by the thermal balance method. EnergyPlus makes common systems and configurations into modules, which is more convenient for users to choose and operate. It can simulate energy consumption by inputting the weather file, the architecture design parameters, the schedules of people, air conditioning, lighting, equipment and other information. The step size of building energy consumption simulation can be adjusted according to the actual demand. In addition, EnergyPlus can be called by grasshopper for building energy simulation. It has an advantage in the simulation of nonlinear building energy consumption and meets the needs of the development of energy-saving design.

2.3.2. The Calculation of Construction Cost

The construction cost is composed of direct fee, overheads, profit and tax. The direct fee, which is used to form or to help form the engineering entity directly during construction period, is composed of direct engineering fee and measure fee. The direct engineering fee is composed of the fees of labor, materials and construction machinery. As the other fees vary greatly by the influence of objective factors, such as enterprise management fees, measure expenses and taxes, the costs of these parts are difficult to be determined. Thus, the construction cost in this study was the comprehensive unit price of building engineering, which is composed of direct engineering fee and profit as shown in Equation (2):

$$C = C_{lab} + C_{mat} + C_{mac} + C_{pro} \quad (2)$$

where C is the comprehensive unit price (thousand yuan), C_{lab} is the labor cost (thousand yuan), C_{mat} is the material cost (thousand yuan), C_{mac} is the construction machinery cost (thousand yuan), C_{pro} is the profit (thousand yuan).

2.4. The Reference Building

2.4.1. Building Form Parameters

According to the surveys, the plane of office buildings in severe cold regions is mostly rectangular. The long side of the building is mostly 48m and the short side of the building is mostly 18 m. These data account for more than 50% of the total survey data respectively. Therefore, the floor area of the reference building in this paper was 900 m² and the height of the internal storey was 3.6 m, which is the typical value for office building in severe cold regions. Six variables were used to control the reference building form. Table 2 showed the variables and the ranges of the variables [45]. Figure 2 illustrated three case models used in this study.

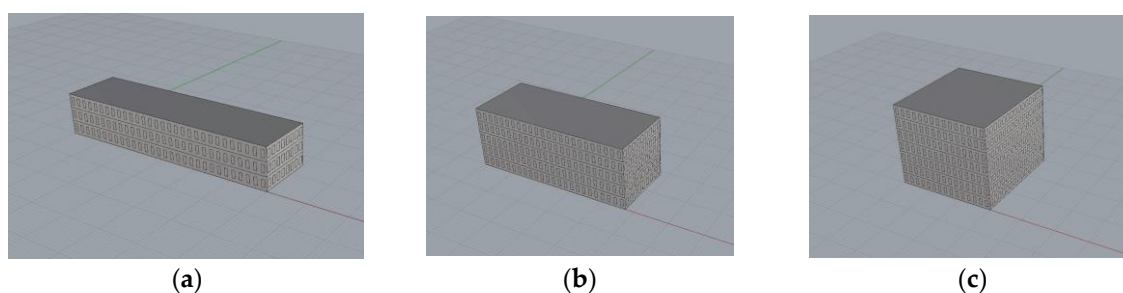


Figure 2. Three case models used in this study. (a) The case model with large aspect ratio. (b) The case model with medium aspect ratio. (c) The case model with small aspect ratio.

Table 2. The range of parameter setting for building form variables.

Variable	Range
Aspect ratio (length/width)	1–4
North window–wall ratio	0.2–0.8
South window–wall ratio	0.2–0.8
East window–wall ratio	0.2–0.8
West window–wall ratio	0.2–0.8
Number of floors	1–7

2.4.2. Construction Parameters

In this study, the structure of the main body of the building was constructed by CLT. Figures 3 and 4 showed the details of exterior wall and roof of the reference buildings. External insulating systems were used in exterior wall and roof of the reference building. These were both composed

of protective layer, insulation layer, structural layer and finish layer. The materials and thickness of insulation layer and the thickness of structural layer of exterior wall can be changed under different situations. The thickness of roof structural layer was greatly affected by structural mechanics, so its thickness was determined as 264 mm [1].

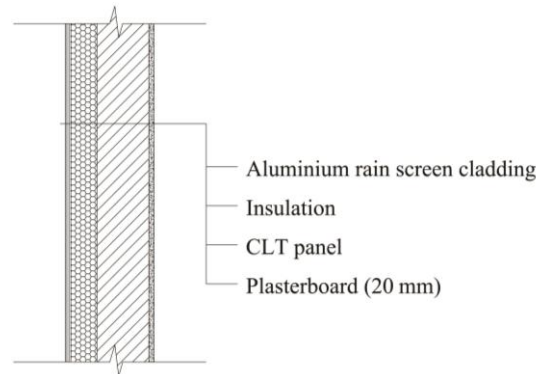


Figure 3. The structural system for exterior walls.

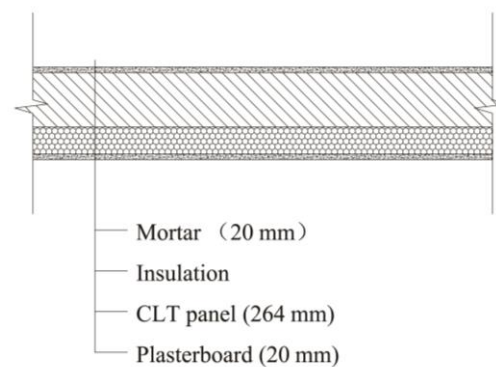


Figure 4. The structural system for roofs.

According to the survey, the exterior wall insulation materials of office buildings in severe cold regions include expanded polystyrene, extruded polystyrene and rock wool. The common thickness of exterior wall insulation layer is between 80 mm and 120 mm. The roof insulation materials of office building in cold area include expanded polystyrene, extruded polystyrene and glass wool, of which thicknesses are between 80 mm and 170 mm. In addition, the thickness of structural layer of exterior wall is between 200–300 mm.

Based on the data, the ranges of model structural layers' thickness were determined. Tables 3 and 4 showed the scopes of thicknesses and the materials of structural layers of the building envelopes in this study. The thickness of structural layer of exterior wall ranged from 60 mm to 500 mm, which is restricted by the capacity of the CLT panels. The ranges of all variables cover the ranges of the usual setting of the office building envelope in severe cold regions.

Table 3. The ranges of structural layers' thickness of building envelope.

Variable	Range
Thickness of exterior wall insulation layer	0–200 mm
Thickness of roof insulation layer	0–200 mm
Thickness of exterior wall structural layer	60–500 mm

Table 4. The materials of structural layers of building envelope.

Variable	Material
Exterior wall insulation material	Expanded polystyrene Extruded polystyrene Rock wool
Roof insulation material	Expanded polystyrene Extruded polystyrene Glass wool

2.4.3. Other Boundary Conditions

The occupancy schedule of the reference building was from 9:00 to 17:00, and there were 2 h for lunch, from 11:00 to 13:00. However, the running time of air conditioning was longer to keep the indoor environment comfortable. The power of equipment system would decrease at lunchtime. In addition, while there was no one coming to work during the holiday, the air conditioning system should still be running during the holidays to ensure a certain indoor temperature to protect the heating pipes and so on. The ideal air-conditioning system is used in this study. The air loop, water loop, and other initial setting of air conditioning are not redefined. Figure 5 illustrated the schedules of air-conditioning. Figures 6–8 illustrated the schedules of lighting, equipment and occupancy condition in the office building respectively. Tables 5–7 showed the loads boundary conditions of the simulation model.

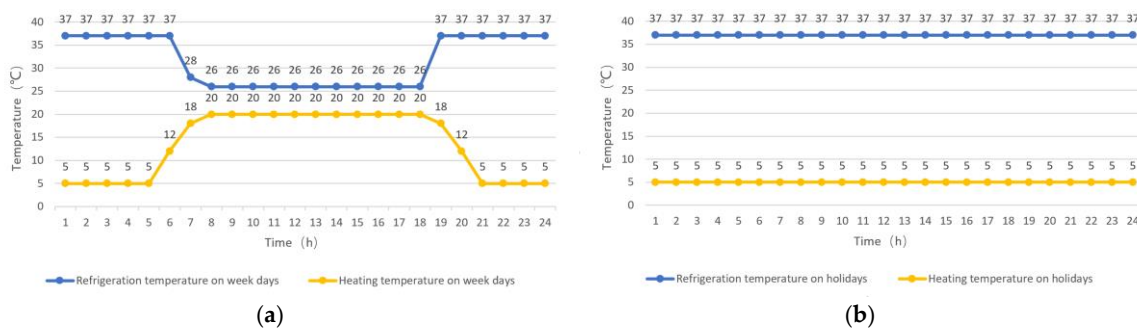


Figure 5. Schedules of air-conditioning. (a) The schedule of air-conditioning on week days; (b) The schedule of air-conditioning on holidays.

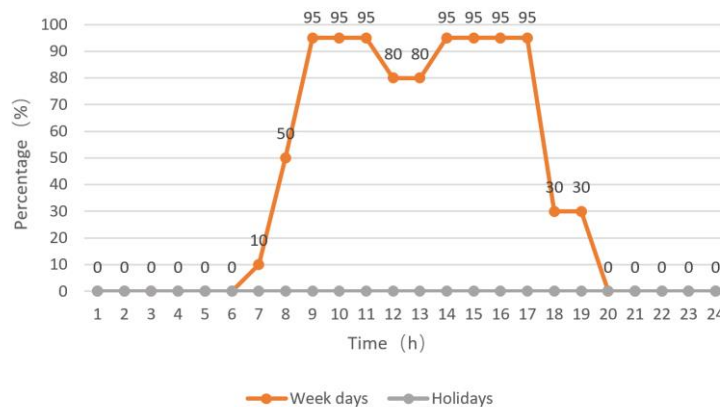


Figure 6. The schedule of lighting.

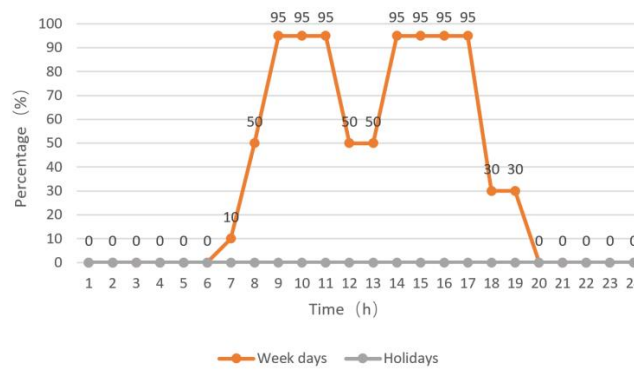


Figure 7. The schedule of equipment.

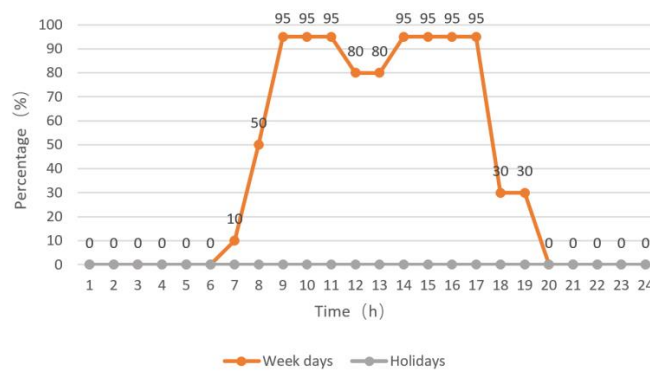


Figure 8. The schedule of occupancy condition.

Table 5. Thermal parameters of non-transparent materials.

Material	Density	Conductivity	Specific Heat
Expanded polystyrene	18 (kg/m ³)	0.041 (W/m·k)	2414.8 (J/kg·k)
Extruded polystyrene	25 (kg/m ³)	0.03 (W/m·k)	5346.4 (J/kg·k)
Rock wool	80 (kg/m ³)	0.05 (W/m·k)	1220 (J/kg·k)
Glass wool	148 (kg/m ³)	0.037 (W/m·k)	1340 (J/kg·k)
CLT	471 (kg/m ³)	0.13 (W/m·k)	1600 (J/kg·k)
Plaster	1050 (kg/m ³)	0.33 (W/m·k)	1050 (J/kg·k)
Aluminum	2700 (kg/m ³)	203 (W/m·k)	920 (J/kg·k)

Table 6. Thermal parameters of transparent material.

Material	Conductivity	Solar Heat Gain Coefficient	Transmittance
Triple glazing window	2 (W/m·k)	0.739	0.7

Table 7. Loads conditions.

Boundary Condition	Value
Power density of lighting	9 (W)
Power density of equipment	15 (W)
Power density of people	10 (m ² /person)

In the process of cost calculation, the amount of material and labor required for each building structure were obtained through the local building standard. The prices of materials come from the data published by the government and the network investigation [46]. Table 8 showed the construction cost of materials.

Table 8. The construction cost of materials.

Construction Material	Cost
CLT	5593.25 (yuan/m ³)
Insulation layer of expanded polystyrene on roof	353.18 (yuan/m ³)
Insulation layer of extruded polystyrene on roof	576.11 (yuan/m ³)
Insulation layer of glass wool on roof	393.23 (yuan/m ³)
Insulation layer of expanded polystyrene for exterior wall	1179.81 (yuan/m ³)
Insulation layer of rock wool for exterior wall	1287.93 (yuan/m ³)
Insulation layer of extruded polystyrene for exterior wall	1362.01 (yuan/m ³)
Mortar	169.52 (yuan/m ³)
Plasterboard	43.75 (yuan/m ²)
Aluminum plate	40.428 (yuan/m ²)
Triple glazing window	299.57 (yuan/m ²)

2.5. Training and Correction of ANN

Latin hypercube sampling (LHS) is used for training data sampling in this study. Compared with the Monte Carlo method, LHS can achieve the same effect with less sampling [47]. LHS divided the parameters of each input variable into many parts and ensured that each part has the same probability to be selected, which is useful to get a more uniform distribution of samples than the Monte Carlo method where the probability of sample extraction near the mean is larger than near both ends.

Therefore, based on the model established in this paper, 500 groups of experimental data were extracted by LHS. The training data in this paper exceeds the minimum number for the training data which is calculated by Equations (3) and (4) [48]:

$$n_h = 2n_i + 1 \quad (3)$$

where n_h is the maximum number of neurons in hidden layer, n_i is the number of input variables;

$$n_d = \left(n_h - \frac{n_i + n_o}{2} \right)^2 \quad (4)$$

where n_d is the minimum number of the training data, n_o is the number of neurons in the output layer.

Then, the distribution of ANN training data should be determined. The range of each parameter was divided into several parts, and the number of samples in each part was compared. The distribution of samples can be determined by this method. After that, building energy consumption simulation and envelope construction cost calculation were carried out for the 500 groups of experiments.

In addition, ANN was established by the results of calculation and simulation. The data which were used for ANN training were randomly divided into training data, validation data and test data according to the proportion of 70:15:15. The ANN training process is terminated when the number of epochs reached the maximum number or the MSE continuous increases 6 times. The maximum number of epochs was set to 1000.

Then, the training effects of ANN with single output variable and multiple output variables were compared. Furthermore, the prediction accuracies of ANN whose neurons in hidden layer are 5, 10, 15 and 20 respectively were analyzed. Finally, the ANN with the best prediction effect was proposed.

3. Results and Discussion

3.1. The Results of Latin Hypercube Sampling

The insulation materials and the floors of the building are not continuous linear variables. Thus, the insulation materials were divided into one part according to each material and the floors of the building were divided into one part according to one layer. Other continuous linear variables were

divided into 10 parts according to their range of values. Figures 9–11 showed the sample distribution of each variable.

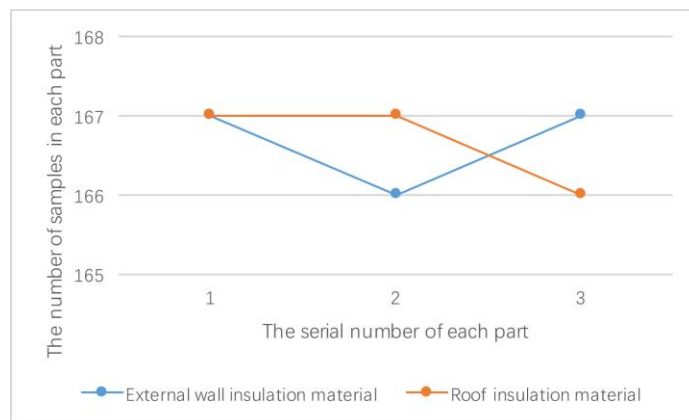


Figure 9. The sample distribution of insulation material variables.

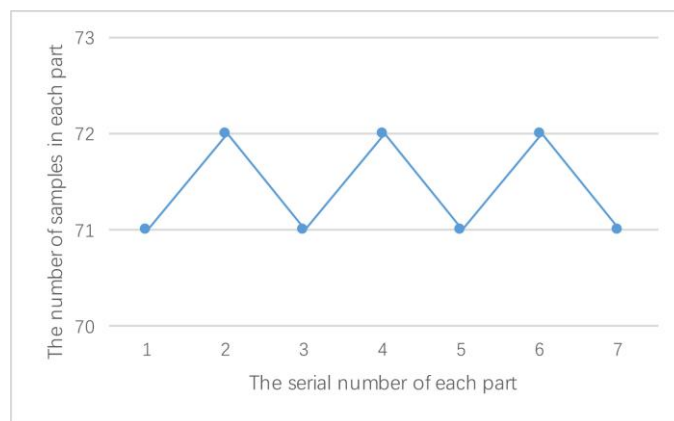


Figure 10. The sample distribution of the number of floors variable.

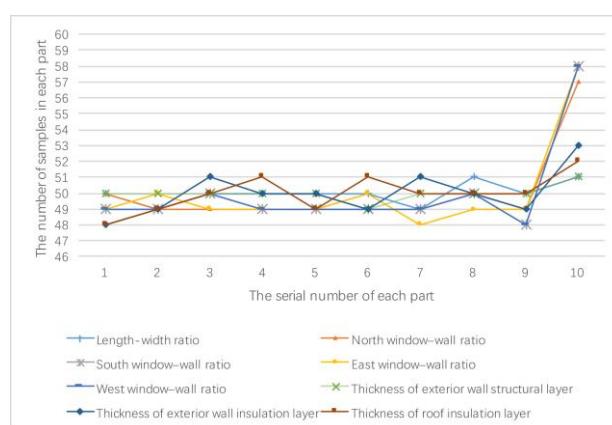


Figure 11. The sample distribution of continuous linear variables.

According to the distribution of samples, the results of LHS were satisfactory. The samples were evenly distributed in all parts of each variable whether it was a continuous linear variable or not. While the sample size of tenth parts of continuous linear variable was larger than that of other parts as the value of the tenth parts was larger than the other nine.

3.2. The Comparing Results of ANNs with Different Output Variables

The output variables of the ANN were building energy consumption and the cost. However, the ANN can predict either single variable or multiple variables at the same time. Therefore, the prediction effects of ANNs with different output variables were compared in this paper to get the better prediction effects.

3.2.1. The ANN with Single Output Variable

Firstly, the performance of ANN with energy consumption as output variable were presented in Figure 12. The training process was terminated at the 17th epoch. The regression R values of training, validation and test data were 0.9916, 0.9622 and 0.9615, and the regression R value of all data was 0.9833. The MSE was 1.5858. In addition, the error distribution of most forecasts was between -1.727 and 1.495 , satisfying the normal distribution characteristic.

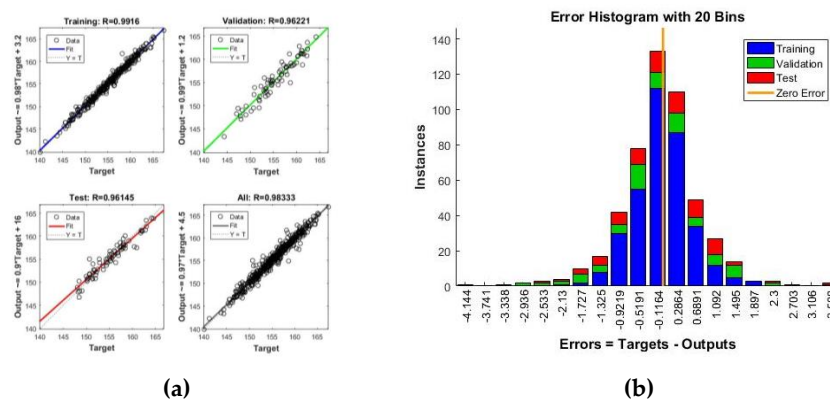


Figure 12. Training results of the ANN with energy consumption as output variable. (a) The regression R values of training; (b) The distribution of training error.

Then, the ANN training was carried out again by changing the output variable to the construction cost. Figure 13 illustrated the results of the ANN training. The training process was terminated at the 19th epoch. The regression R values of training, validation and test data were 0.9975, 0.9934 and 0.9964, and the regression R value of all data was 0.9968. The MSE was 0.0176. The error distribution of most forecasts was between -0.1229 and 0.1057 .

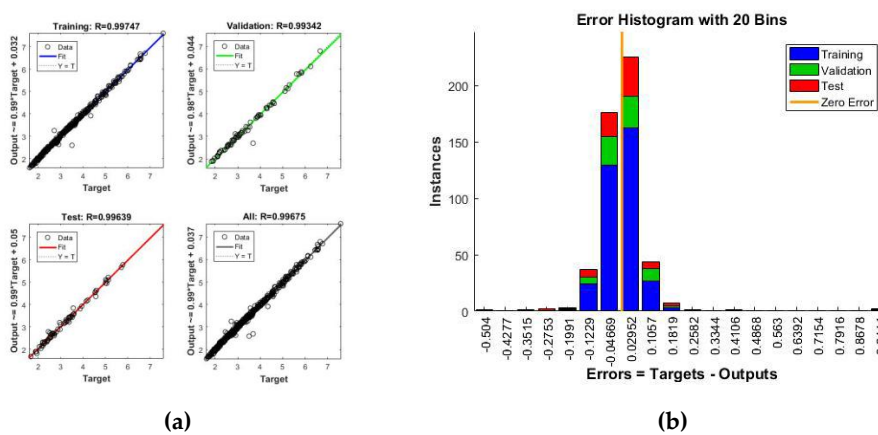


Figure 13. Training results of the ANN with construction cost as output variable. (a) The regression R values of training; (b) The distribution of training error.

3.2.2. The ANN with Multiple Output Variables

Figure 14 illustrated the training results of the ANN with energy consumption and construction cost as output variables. The training process was terminated at the 38th epoch. All the R values were higher than the R values of ANNs with single output. The regression R values of training, validation and test data were 0.9996, 0.9997 and 0.9988, and the regression R value of all data was 0.9995. The MSE is 1.957×10^3 . In addition, the distribution of errors was more concentrated than the previous results. To summarize, the ANN with multiple output variables should be applied to predict energy consumption and cost of CLT office buildings in severe cold regions.

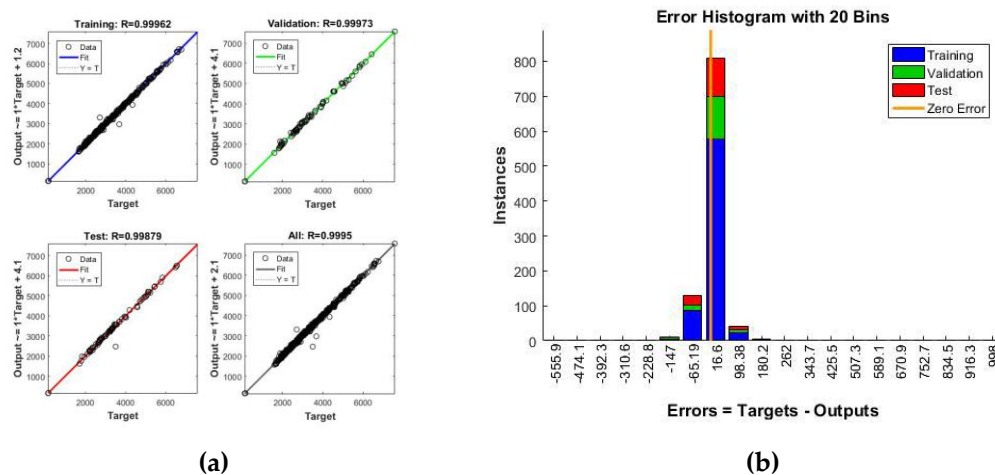


Figure 14. Training results of the ANN with multiple output variables; (a) The regression R values of training. (b) The distribution of training error.

3.3. The Comparing Results of ANNs with Different Number of Hidden Layer Neurons

The influences of the number of neurons in hidden layer on ANN were analyzed. The number of hidden layer neurons were set as 5, 15 and 20 respectively. The training process were terminated at the 34th, 12th and 17th epoch. Table 9 showed the results of the performances of ANNs with different number of neurons in hidden layer.

Table 9. The performances of the ANNs with different number of neurons in hidden layer.

The Number of Hidden Layer Neurons	R Value of Training	R Value of Validation	R Value of Test	R Value of All Data	MSE
5	0.9986	0.9978	0.9986	0.9985	1.552×10^4
10	0.9996	0.9997	0.9988	0.9995	1.957×10^3
15	0.9994	0.9994	0.9991	0.9993	3.721×10^3
20	0.9996	0.9990	0.9994	0.9995	6.469×10^3

The performances of ANN with five neurons in the hidden layer were worse than others. The regression R values were smaller and the value of MES was greater. In addition, the R values of the ANN with 10 neurons in the hidden layer was similar to the R values with 15 and 20 neurons, but the best was the ANNs with 10 hidden layer neurons. Thus, it is concluded that the number of hidden layer neurons in this study should be set as 10 and the best MSE is 1.957×10^3 .

4. Conclusions

In this paper, an ANN was established to predict the energy consumption and cost of the CLT office buildings in severe cold regions. The proper sampling method, output variables and the number of neurons in the hidden layer were all determined by a series of analyses. The main conclusions of this study were as follows:

- The LHS method can guarantee the homogeneity of the samples and be competent for the sampling work of the ANN training data.
- The ANN with multiple output variables has better prediction performance than the ANN with single output variable when predicting the energy consumption and cost of CLT office buildings in severe cold regions.
- For the ANN established in this paper, the number of hidden layer neurons in ANN should be greater than 5 and the best is 10. The best MSE is 1.957×10^3 .
- The time of predicting building energy consumption and cost by ANN is 80% shorter than that of traditional building energy consumption simulation and cost calculation methods.

Acknowledgments: This research is supported by National Natural Science Foundation of China (NSFC: 51578172), the China National Key R&D Program (Grant No. 2016YFC0700209), Science and Technology Funds of the Ministry of Housing and Urban-Rural Development of the China (2016-K1-001) and Research Funds of The Architectural Society of China (2014-01).

Author Contributions: Kai Xing and Hongrui Zhang conceived and designed the experiments; Hongrui Zhang performed the experiments; Qi Dong and Hongrui Zhang analyzed the data; Kai Xing contributed reagents/materials/analysis tools; Qi Dong wrote the paper.

Conflicts of Interest: The authors declare no conflicts of interest.

Nomenclature

ANN	Artificial neural network
CLT	Cross laminated timber
LHS	Latin hypercube sampling
MSE	Mean square error
BP	Back propagation
E	Total energy consumption (kW·h/m ²)
E _{he}	Heating energy consumption (kW·h/m ²)
E _{co}	Cooling energy consumption (kW·h/m ²)
E _{eq}	Equipment energy consumption (kW·h/m ²)
E _{li}	Lighting energy consumption (kW·h/m ²)
C	Comprehensive unit price (thousand yuan)
C _{lab}	Labor cost (thousand yuan)
C _{mat}	Material cost (thousand yuan)
C _{mac}	Construction machinery cost (thousand yuan)
C _{pro}	Profit (thousand yuan)
n _h	The maximum number of neurons in hidden layer
n _d	The minimum number of the training data
n _i	The number of input variables
n _o	The number of output variables

References

1. Guo, H.; Liu, Y.; Chang, W.S.; Shao, Y.; Sun, C. Energy Saving and Carbon Reduction in the Operation Stage of Cross Laminated Timber Residential Buildings in China. *Sustainability* **2017**, *9*, 292. [[CrossRef](#)]
2. Li, Y.; Yao, J.; Li, R.; Zhang, Z.; Zhang, J. Thermal and energy performance of a steel-bamboo composite wall structure. *Energy Build.* **2017**, *156*, 225–237. [[CrossRef](#)]
3. Tian, W.; Song, J.; Li, Z.; Wlode, P.D. Bootstrap techniques for sensitivity analysis and model selection in building thermal performance analysis. *Appl. Energy* **2014**, *135*, 320–328.
4. Ürge-Vorsatz, D.; Novikova, A. Potentials and costs of carbon dioxide mitigation in the world's buildings. *Energy Policy* **2008**, *36*, 642–661. [[CrossRef](#)]
5. Pérez-Lombard, L.; Ortiz, J.; Pout, C. A review on buildings energy consumption information. *Energy Build.* **2008**, *40*, 394–398. [[CrossRef](#)]

6. Liu, G.; Wu, Z.; Hu, M. Energy Consumption and Management in Public Buildings in China: An Investigation of Chongqing. *Energy Procedia* **2012**, *14*, 1925–1930. [[CrossRef](#)]
7. Sadineni, S.B.; Madala, S.; Boehm, R.F. Passive building energy savings: A review of building envelope components. *Renew. Sustain. Energy Rev.* **2011**, *15*, 3617–3631. [[CrossRef](#)]
8. Braulio-Gonzalo, M.; Bovea, M.D. Environmental and cost performance of building's envelope insulation materials to reduce energy demand: Thickness optimisation. *Energy Build.* **2017**, *150*, 527–545. [[CrossRef](#)]
9. Gustavsson, L.; Joelsson, A. Life cycle primary energy analysis of residential buildings. *Energy Build.* **2010**, *42*, 210–220. [[CrossRef](#)]
10. Vilguts, A.; Serdjuks, D.; Pakrastins, L. Design Methods of Elements from Cross-laminated Timber Subjected to Flexure. *Procedia Eng.* **2015**, *117*, 10–19. [[CrossRef](#)]
11. Mallo, M.F.L.; Espinoza, O. Awareness, perceptions and willingness to adopt Cross-Laminated Timber by the architecture community in the United States. *J. Clean. Prod.* **2015**, *94*, 198–210. [[CrossRef](#)]
12. Hadden, R.M.; Bartlett, A.I.; Hidalgo, J.P.; Santamaria, S.; Wiesner, F.; Bisby, L.A.; Bisby, L.A.; Deeny, S.; Lane, B. Effects of exposed cross laminated timber on compartment fire dynamics. *Fire Saf. J.* **2017**, *91*, 480–489. [[CrossRef](#)]
13. Fragiacommo, M.; Dujic, B.; Sustersic, I. Elastic and ductile design of multi-storey crosslam massive wooden buildings under seismic actions. *Eng. Struct.* **2011**, *33*, 3043–3053. [[CrossRef](#)]
14. Warren, H.; Manbeck, H.B.; Janowiak, J.J.; Witmer, R.W.J. Differences in LRFD and ASD outcomes for hardwood glued-laminated bridges. *Am. Soc. Agric. Eng.* **1998**, *41*, 803–811. [[CrossRef](#)]
15. Lineham, S.A.; Thomson, D.; Bartlett, A.I.; Bisby, L.A.; Hadden, R.M. Structural response of fire-exposed cross-laminated timber beams under sustained loads. *Fire Saf. J.* **2016**, *85*, 23–34. [[CrossRef](#)]
16. Kovacic, I.; Waltenbereger, L.; Gourelis, G. Tool for life cycle analysis of facade-systems for industrial buildings. *J. Clean. Prod.* **2016**, *130*, 260–272. [[CrossRef](#)]
17. Yang, M.D.; Lin, M.D.; Lin, Y.H.; Tsai, K.T. Multiobjective optimization design of green building envelope material using a non-dominated sorting genetic algorithm. *Appl. Therm. Eng.* **2017**, *111*, 1255–1264. [[CrossRef](#)]
18. Valdiserri, P.; Biserni, C. Energy performance of an existing office building in the northern part of Italy: Retrofitting actions and economic assessment. *Sustain. Cities Soc.* **2016**, *27*, 65–72. [[CrossRef](#)]
19. Valdiserri, P.; Biserni, C.; Tosi, G.; Garai, M. Retrofit Strategies Applied to a Tertiary Building Assisted by Trnsys Energy Simulation Tool. *Energy Procedia* **2015**, *78*, 765–770. [[CrossRef](#)]
20. Song, X.; Ye, C.; Li, H.; Wang, X.; Ma, W. Field study on energy economic assessment of office buildings envelope retrofitting in southern China. *Sustain. Cities Soc.* **2017**, *28*, 154–161. [[CrossRef](#)]
21. Gustafsson, M.; Dipasquale, C.; Poppi, S.; Bellini, A.; Fedrizzi, R.; Bales, C.; Ochs, F.; Sié, M.; Holmberg, S. Economic and environmental analysis of energy renovation packages for European office buildings. *Energy Build.* **2017**, *148*, 155–165. [[CrossRef](#)]
22. Balionis, E.; Migilinskas, D.; Džiugaitė-Tumėnienė, R. The Multicriteria Assessment of Multi-storey Office Building Energy Performance. *Procedia Eng.* **2017**, *172*, 83–87. [[CrossRef](#)]
23. Kumar, R.; Aggarwal, R.K.; Sharma, J.D. Energy analysis of a building using artificial neural network: A review. *Energy Build.* **2013**, *65*, 352–358. [[CrossRef](#)]
24. Fumo, N. A review on the basics of building energy estimation. *Renew. Sustain. Energy Rev.* **2014**, *31*, 53–60. [[CrossRef](#)]
25. Ascione, F.; Bianco, N.; Stasio, C.D.; Mauro, G.M.; Vanoli, G.P. CASA, cost-optimal analysis by multi-objective optimisation and artificial neural networks: A new framework for the robust assessment of cost-optimal energy retrofit, feasible for any building. *Energy Build.* **2017**, *146*, 200–219. [[CrossRef](#)]
26. Pino-Mejías, R.; Pérez-Fargallo, A.; Rubio-Bellido, C.; Pulido-Arcas, J.A. Comparison of linear regression and artificial neural networks models to predict heating and cooling energy demand, energy consumption and CO₂ emissions. *Energy* **2017**, *118*, 24–36. [[CrossRef](#)]
27. Wang, Z.; Srinivasan, R.S. A review of artificial intelligence based building energy use prediction: Contrasting the capabilities of single and ensemble prediction models. *Renew. Sustain. Energy Rev.* **2016**, *75*, 796–808. [[CrossRef](#)]
28. Sholahudin, S.; Han, H. Simplified dynamic neural network model to predict heating load of a building using Taguchi method. *Energy* **2016**, *115*, 1672–1678. [[CrossRef](#)]

29. Kalogirou, S.A. Artificial neural networks in renewable energy systems applications: A review. *Renew. Sustain. Energy Rev.* **2001**, *5*, 373–401. [[CrossRef](#)]
30. Deb, C.; Eang, L.S.; Yang, J.; Santamouris, M. Forecasting diurnal cooling energy load for institutional buildings using Artificial Neural Networks. *Energy Build.* **2016**, *121*, 284–297. [[CrossRef](#)]
31. Chou, J.S.; Bui, D.K. Modeling heating and cooling loads by artificial intelligence for energy-efficient building design. *Energy Build.* **2014**, *82*, 437–446. [[CrossRef](#)]
32. Jovanović, R.Ž.; Sretenović, A.A.; Živković, B.D. Ensemble of various neural networks for prediction of heating energy consumption. *Energy Build.* **2015**, *94*, 189–199. [[CrossRef](#)]
33. Paudel, S.; Elmtiri, M.; Kling, W.L.; Corre, O.L.; Lacarrière, B. Pseudo dynamic transitional modeling of building heating energy demand using artificial neural network. *Energy Build.* **2014**, *70*, 81–93. [[CrossRef](#)]
34. Platon, R.; Dehkordi, V.R.; Martel, J. Hourly prediction of a building's electricity consumption using case-based reasoning, artificial neural networks and principal component analysis. *Energy Build.* **2015**, *92*, 10–18. [[CrossRef](#)]
35. Daut, M.A.M.; Hassan, M.Y.; Abdullah, H.; Rahman, H.A.; Abdullah, M.P.; Hussin, F. Building electrical energy consumption forecasting analysis using conventional and artificial intelligence methods: A review. *Renew. Sustain. Energy Rev.* **2017**, *70*, 1108–1118. [[CrossRef](#)]
36. Ascione, F.; Bianco, N.; Stasio, C.D.; Mauro, G.M.; Vanoli, G.P. Artificial neural networks to predict energy performance and retrofit scenarios for any member of a building category: A novel approach. *Energy* **2017**, *118*, 999–1017. [[CrossRef](#)]
37. Tatari, O.; Kucukvar, M. Cost premium prediction of certified green buildings: A neural network approach. *Build. Environ.* **2011**, *46*, 1081–1086. [[CrossRef](#)]
38. Beccali, M.; Ciulla, G.; Brano, V.L.; Galatioto, A.; Bonomolo, M. Artificial neural network decision support tool for assessment of the energy performance and the refurbishment actions for the non-residential building stock in Southern Italy. *Energy* **2017**, *137*, 1201–1218. [[CrossRef](#)]
39. Alshamrani, O.S. Construction cost prediction model for conventional and sustainable college buildings in North America. *J. Taibah Univ. Sci.* **2016**, *11*, 315–323. [[CrossRef](#)]
40. Ruiz, L.G.B.; Rueda, R.; Cuéllar, M.P.; Pegalajar, M.C. Energy consumption forecasting based on Elman neural networks with evolutive optimization. *Exp. Syst. Appl.* **2017**, *92*, 380–389. [[CrossRef](#)]
41. Ahmad, M.W.; Mourshed, M.; Rezgui, Y. Trees vs Neurons: Comparison between random forest and ANN for high-resolution prediction of building energy consumption. *Energy Build.* **2017**, *147*, 77–89. [[CrossRef](#)]
42. Martellotta, F.; Ayr, U.; Stefanizzi, P.; Sacchetti, A.; Riganti, G. On the use of artificial neural networks to model household energy consumptions. *Energy Procedia* **2017**, *126*, 250–257. [[CrossRef](#)]
43. Li, K.; Hu, C.; Liu, G.; Xue, W. Building's electricity consumption prediction using optimized artificial neural networks and principal component analysis. *Energy Build.* **2015**, *108*, 106–113. [[CrossRef](#)]
44. Huang, D.; He, S.; He, X.; Zhu, X. Prediction of wind loads on high-rise building using a BP neural network combined with POD. *J. Wind Eng. Ind. Aerodyn.* **2017**, *170*, 1–17.
45. Tian, W.; Yang, S.; Zuo, J.; Li, Z.Y.; Liu, Y.L. Relationship between built form and energy performance of office buildings in a severe cold Chinese region. *Build. Simul.* **2017**, *10*, 11–24. [[CrossRef](#)]
46. Material Price of Construction Engineering. Available online: http://www.lnzj.com.cn/jgxx_cl.asp (accessed on 27 November 2017).
47. Novák, D.; Lehký, D. ANN inverse analysis based on stochastic small-sample training set simulation. *Eng. Appl. Artif. Intell.* **2006**, *19*, 731–740. [[CrossRef](#)]
48. Biswas, M.A.R.; Robinson, M.D.; Fumo, N. Prediction of residential building energy consumption: A neural network approach. *Energy* **2016**, *117*, 84–92. [[CrossRef](#)]

